

# Comparison of hexagonal and square dot centers for EP halftones

*Mila Turbek, Steve Weed, Tomasz Cholewo, Brian Damon, Michael Lhamon  
Lexmark International, Inc.  
Lexington, KY, USA*

## Abstract

Hexagonal dot packing seems to offer benefits for halftone printing compared to conventional square dot packing, but little practical experience has been reported. Taking advantage of recent refinements in digital electrophotographic (EP) printer technology, the authors conducted experiments on a commercially deployable system to assess whether the potential advantages of hexagonal dot packing are economically exploitable.

Keywords: hexagonal, halftone, spot function, spectrogram

## Introduction

Digital printing has nearly always been accomplished by round dots organized on rectangular grids. It is understood that the improved packing efficiency of hexagonal grids for round dots would be more easily achieved than rectangular dots for rectangular grids, but evidently neither hexagonal grids nor rectangular dots have generally been considered worthwhile.

Ulichney [1] addressed halftone theory for hexagonal grids. Average dot overlap can be reduced, since smaller dots can ensure 100 percent coverage for the same dot frequency. In addition, as Harrington [2] noted, each dot has only six instead of eight dots with which to overlap, which should simplify halftone pattern analysis.

This report compares some halftones for hexagonal dot packing with comparable screens for square dot packing and demonstrates some implications for image quality, tone reproduction and halftone formation patterns. Two hypotheses are investigated for hexagonal dot packing:

- gray levels are more usefully distributed for the same cluster size;
- important screen frequencies and angles concentrate less visually perceptible artifact energy.

An important effect in EP printers is that dots are modulated by the proximity of other dots. Results will be analyzed for whether this proximity effect is exacerbated or attenuated by having all overlapping dots more equidistant. The greater interdependency of dots in the same raster line

compared to dots on adjacent raster lines can be a confounding effect.

Hexagonal packing was implemented on the test printer by shifting the dot centers in alternate raster lines by half of the dot spacing. In Ulichney's terminology, the resulting aspect ratio,  $\alpha$ , was 1, while the ideal aspect ratio for round dots would have been  $2/\sqrt{3}$  or  $2\sqrt{3}$ . Neither optimizing the dot shape and size for  $\alpha = 1$  nor optimizing  $\alpha$  for the given dot shape and size were investigated in this study.

## Euclidean screen for square dot array

To create a basis for comparison, the printer was first exercised using a conventional Euclidean spot function generated for a rectangular dot array, as in Figure 1. Since the Euclidean halftone is well-known [3], interested readers should be able to bridge from our analyses to others with which they may be familiar.

At viewing distances typical for letters, dot clusters large enough to closely approximate the ideal shapes for the Euclidean spot function have a very apparent periodic structure when printed at 600 dpi.

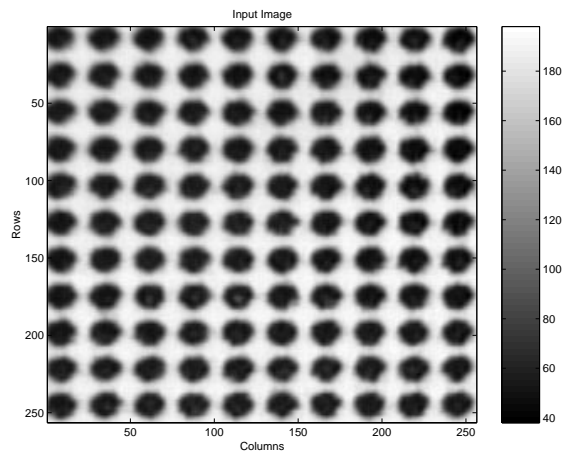


Figure 1: Magnified image of a coarse 0 degree Euclidean spot function designed for square dot packing at about 42 percent requested coverage.

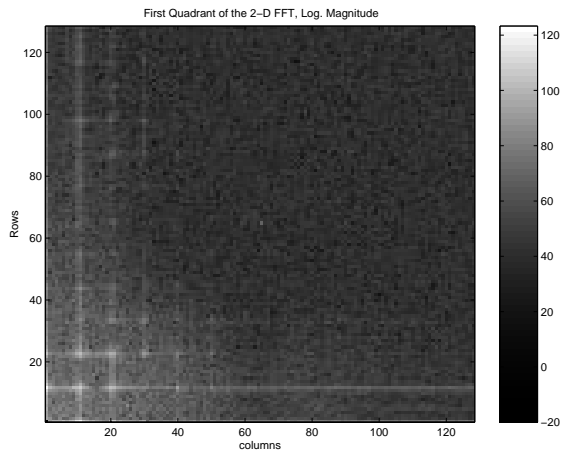


Figure 2: First quadrant of 2D FFT for 0 degree Euclidean spot function designed for square dot packing at about 42 percent requested coverage.

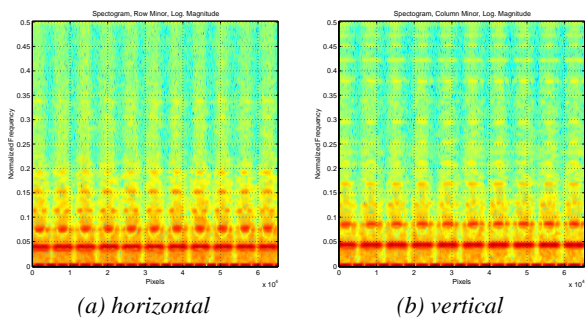


Figure 3: Spectrograms for 0 degree Euclidean spot function designed for square dot packing at about 42 percent requested coverage.

Spectrograms allow easy correlation of periodic energy with location and are particularly useful when this energy is not uniformly distributed [4]. However, even though halftones were regularly periodic for the images in this study, the two-dimensional FFT (Figure 2) still seems to be relatively uninformative in comparison to spectrograms (Figure 3). Consequently, spectrograms were used for halftone frequency analysis in this study.

Spectrogram analyses were performed on  $256 \times 256$  pixel gray images captured from a video camera and StereoZoom 7 microscope. Unfortunately, this video camera does not have ‘square’ pixels; at lowest magnification, the camera captures an 8 mm square area in  $413 \times 382$  pixels. Since the 0 degree Euclidean spot function of Figure 1 has the same periodic structure in the vertical and horizontal directions, its row and column spectrograms in Figure 3 are nearly identical, allowing for image aspect ratio.

The advantages of hexagonal packing should be greater

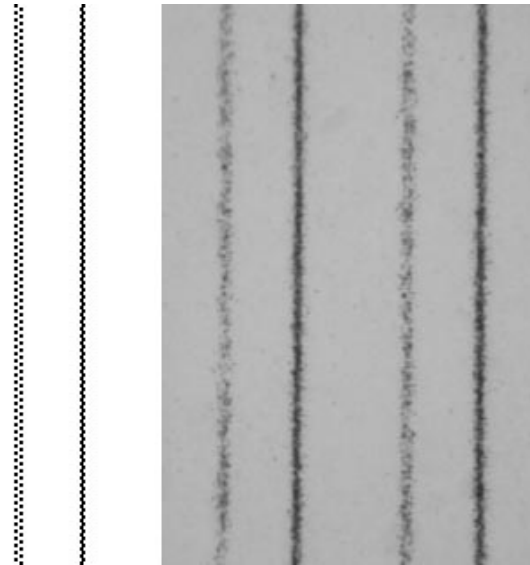


Figure 4: On the left: ideal two-dot-wide 50 percent checkerboard bitmaps, shifted for hexagonal dot packing. On the right: magnified view of an actual print. A similar pattern was used to ensure that halftone tiles for hexagonal packing were in phase with the dot offset.

for small dot clusters associated with higher effective line screens. Using a threshold array composed of multiple small dot clusters, such as Lexmark’s PictureGrade, is one technique for obtaining more gray levels while attenuating low frequency energy. These analyses focused on single cluster arrays that could be aggregated for real applications. A threshold array designed for hexagonal dot packing will generally need to tile without changing phase of raster line shift and consequently needs to be an even number of raster lines in height.

An important halftone metric is how usefully distributed are gray levels for the real printer with a given number of dots in a cluster. It was anticipated that, since hexagonal packing results in fewer immediate neighbors to provoke EP dot size modulation, more light gray levels should be available.

The next part of the experiment verified microcode for packing dots in hexagonal array, which is nearly an act of faith, since a half-dot offset is unobvious by direct observation of magnified symmetric bitmap patterns. For example, vertical lines printed with hexagonal dot packing (alternate raster lines printed with one-half dot horizontal offset) were indistinguishable from vertical lines printed with square dot packing on the same mechanism. However, consider the bitmaps in Figure 4, of two mirror-image vertical 50 percent checkerboards, each two pixels wide. With hexagonal dot packing, one of the checkerboard patterns is printed with a net one-half dot offset between adja-

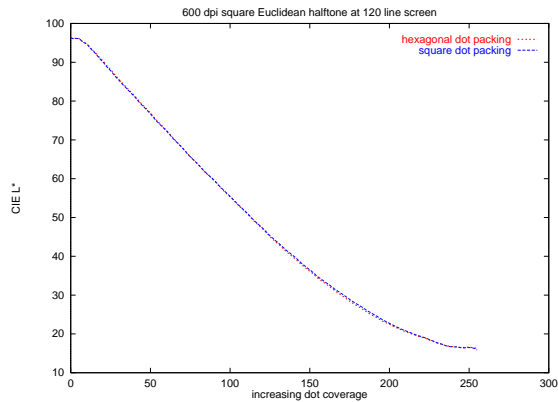


Figure 5: Gray values for 0 degree  $5 \times 5$  Euclidean spot function designed for square dot packing, printed at 600 dpi with hexagonal and square dot packing.

cent dots, while the other has a net 1.5 dot offset between adjacent dots. Through the magic of laser electrophotographic printer technology, the resulting prints (Figure 4) are distinguishable from straight vertical lines to the unaided eye primarily in that the line with net 1.5 dot offsets has reduced density. In fact, edge raggedness was comparable for vertical straight lines printed with alternating one-half horizontal dot offsets for hexagonal dot packing and vertical lines printed with square dot packing. ImageXpert [5] edge raggedness measurements for printed vertical lines ranged from 0.010 to 0.023 mm, using the square dot packing for which it was designed. Comparable measurements using hexagonal dot packing ranged from 0.013 to 0.026 mm. This was good news, because significantly degrading the quality of lines in exchange for refined halftone performance would be an unacceptable compromise. It is possible that taking further advantage of hexagonal dot packing by reducing dot size could increase edge raggedness.

For most bitmaps printed with both square and hexagonal dot packing, any detectable differences between prints were generally in density of high frequency patterns. These density changes are presumably driven by dot size modulation from changes in distance between dots on adjacent raster lines. Unfortunately, as with vertical lines, half-dot shifts were not directly observable in magnified images of the investigated halftone patterns.

Using the threshold array designed for square dot packing with the printer configured for hexagonal packing slightly improved lighter tones for the 0 degree Euclidean screen. Horizontally shifting alternating centers of vertically aligned spots slightly increases the distance between them, which would tend to decrease the size of those spots. This effect depends on vertical cell spacing that corresponds to an odd number of raster lines and does not gen-

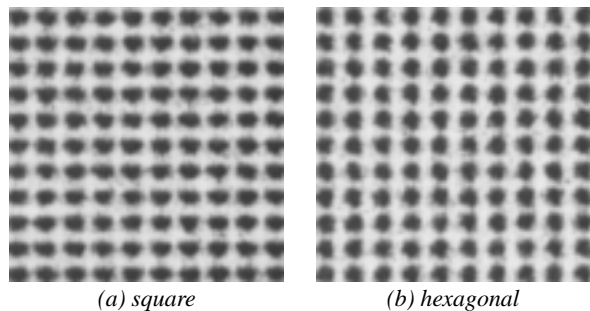


Figure 6: Magnified images of 100 lpi screens for 0 degree Euclidean spot functions printed at 600 dpi.

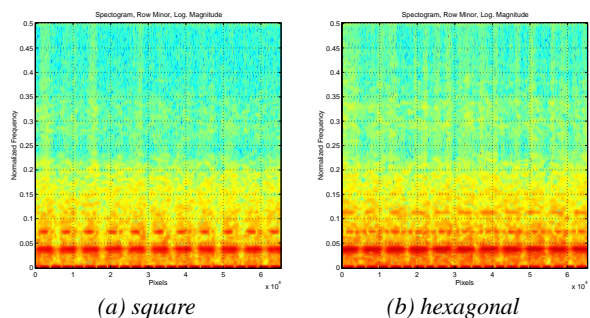


Figure 7: Row spectrograms for 100 lpi 0 degree Euclidean spot functions printed at 600 dpi. The square case (a) shows more first harmonic energy at around 0.07 normalized frequency.

eralize to dark tones or all screen angles. However, since dot gain and overlap typically result in a higher proportion of dark tones than light tones, it is potentially useful. As expected, hexagonal packing has more influence on gray rendition for small threshold arrays, such as  $5 \times 5$  dots (Figure 5).

## Euclidean screen for hexagonal dot array

A threshold array was then generated by the Euclidean spot function based on hexagonal dot packing geometry. For this exercise,  $6 \times 6$  clusters were used, resulting in a 100 line screen. A  $6 \times 6$  Euclidean screen was also generated for square dot packing, so that results could be directly compared (Figure 6). A  $6 \times 6$  halftone cluster provides enough gray levels to avoid contouring on many prints, and halftone periodicity for 100 line screens can be made visible or not, by varying the distance a print is held from the eye. A simple experiment was performed:

1. Using both screens, print a column of gray steps.
2. Overlap the pages so that both columns are visible.
3. Fix on any gray level with the prints held at arm's length.

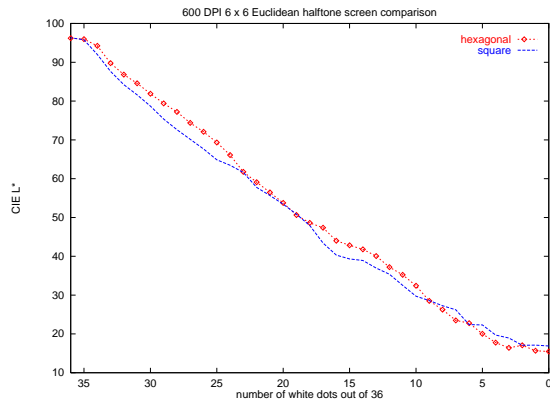


Figure 8: Gray values for 0 degree square and hexagonal Euclidean spot functions, 100 lpi at 600 dpi.

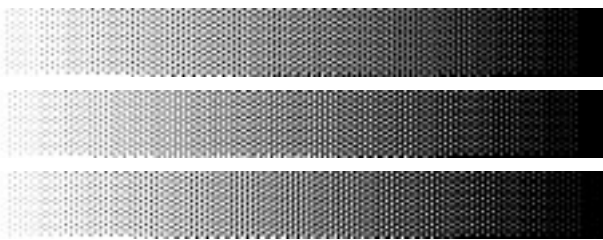


Figure 9: Gradients using coarse idealized Ulichney hexagonal screens. The upper screen is a positive spiral; a negative spiral is in the middle, and a tristate halftone screen is at the bottom.

4. Move the pages closer, until halftone periodicity is just visible for that gray level on only one of the pages.

Our results for this experiment were that the square Euclidean screen was consistently visible before the hexagonal screen. Inspection of the spectrograms suggests that the greater visibility of square Euclidean screens may be largely attributable to higher first harmonic energy (at around 0.07 normalized frequency in Figure 7).

Figure 8 shows that low dot coverage gray levels print lighter for hexagonal Euclidean screen than for square Euclidean, as was hoped.

### Ulichney screens for hexagonal grids

A motivation for applying Euclidean spot function to hexagonal packing was that it readily lent itself to direct comparison with square dot packing. Ulichney described a spiral-dot screen and a tristate ordering scheme that better exploit hexagonal dot packing, which we implemented using  $9 \times 6$  tiles (Figure 9).

Classical spiral-dot screens are designed for ink control in offset presses, where black dots are clustered to improve

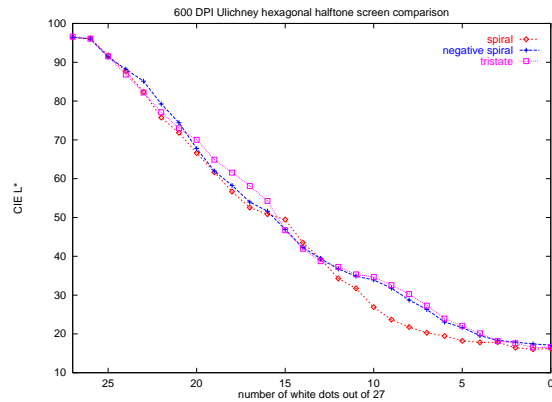


Figure 10: Gray values for Ulichney hexagonal screens.

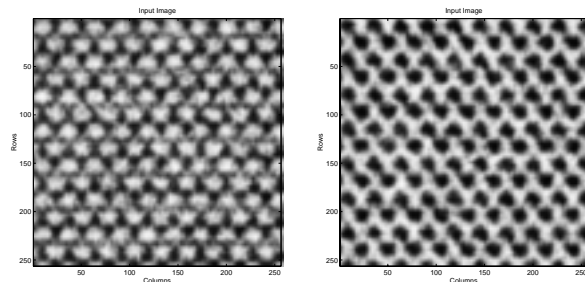


Figure 11: Spiral-dot patterns for 10/27 black dots at 600 dpi.

ink flow control. Laser printers, on the other hand, tend to have more problems with isolated unprinted clusters, so a negative spiral-dot screen produced a better distribution of gray levels, as can be ascertained from Figure 10.

Spiral-dot screens (Figure 11) are different in the vertical and horizontal directions, and their vertical and horizontal spectrograms (Figure 12) are also dissimilar. The spectrograms for negative spiral-dot (not shown) are nearly identical to Figure 12.

Inflection points can be observed in middle grays of lightness plots for both Euclidean (Figure 8) and Ulichney (Figure 10) screens, because the dot clusters abruptly connect and increase in size. This can be addressed by increasing the number of clusters in a tile and sequencing the threshold values among clusters, so that connections occur over a wider range of gray values. This refinement was not attempted for this study. For example, the  $9 \times 6$  tiles used for Ulichney patterns each only had 27 different threshold values.

### Conclusions

Using two versions of microcode, a single electrophotographic printer was configured for either hexagonal or

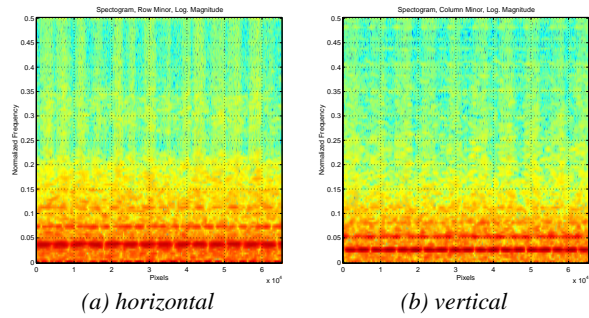


Figure 12: Spectrograms of a positive spiral-dot screen.

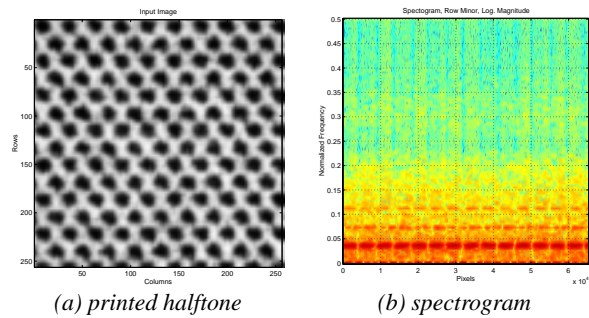


Figure 13: Tristate ordering scheme.

square dot packing at 600 dpi. Consequently, practically all differences in prints could be attributed to this single change. Hexagonal dot packing yielded subtle but useful improvements in gray level distribution. Spatial artifacts for Euclidean screens based on square dot packing were consistently apparent at slightly greater distances than for comparable screens for hexagonal packing. Interestingly, screens designed for hexagonal packing conferred some of these improvements even when printed with square dot packing. Among the Ulichney patterns for hexagonal dot packing, spatial artifacts were more visible in EP prints made with spiral-dot screens than the tristate screen (Figure 13), which also had a better distribution of dark gray levels. Negative spiral-dot had better distribution of gray levels than positive spiral-dot screen, which is presumably at a disadvantage in EP printing because dot overlap too quickly fills in the nearly concentric white space around black dot clusters. Additional experiments with rotated Ulichney hexagonal patterns may be worthwhile.

## References

[1] R. Ulichney. *Digital halftoning*. MIT Press, Cambridge, Massachusetts, 1987.

[2] S. J. Harrington. Three-pixel characterization of hexagonal pixel grids. *Xerox Disclosure Journal*, 23:229–230, Sep/Oct 1998. <http://www.xerox.com/research/xdj/199805/xdj-012.html>.

[3] A. Donnelly. Spot function reference. *Austin Donnelly's Home Page*, 1.3, August 1998. <http://www.cl.cam.ac.uk/~and1000/newsprint/spot-ref.html>.

[4] S. T. Love, S. F. Weed, S. W. Daniel, and M. E. Lhamon. Converting color values using stochastic interpolation. In *IS&T/SPIE's 12th Annual Symposium, Electronic Imaging 2000: Science and Technology*, San Jose, Calif., January 2000.

[5] KDY Inc. ImageXpert automated image quality for printers and plotters. *ImageXpert – Literature*, 2.02:2–12, 1998. [http://www.imagexpert.com/pdf/an\\_ptr.pdf](http://www.imagexpert.com/pdf/an_ptr.pdf).